J. Fluid Mech. (2013), *vol.* 717, *pp.* 193–202.
doi:10.1017/jfm.2012.566

Disintegrating supercritical jets in a subcritical environment

Arnab Roy[1],†, Clement Joly[2] and Corin Segal[1]

[1]Mechanical and Aerospace Engineering Department, University of Florida, Gainesville, FL 32611, USA
[2]Turbulent Combustion, CNRS ICARE, Orléans CEDEX 2, 45071, France

(Received 29 August 2012; revised 12 October 2012; accepted 13 November 2012;
first published online 1 February 2013)

Supercritical fluid injection using a single round injector into a quiescent atmosphere at subcritical and supercritical conditions was studied experimentally with particular attention paid to supercritical-into-subcritical injection and the reassertion of surface tension. The entire system was binary since the surrounding atmosphere consisted of an inert gas of a different composition than that of the injected fluid. Average densities and density gradients were quantified and a method was applied to quantify the resulting drop formation due to the disintegration of the jet based on the experimental conditions. The evolution of drop size with distance from the injector was identified.

Key words: jets, mixing, multiphase flow

1. Introduction

The majority of theories and empirical evaluations of a liquid jet break-up and mixing processes have been developed for a restricted range of experimental conditions where the pressures and temperatures of the surrounding gas are well below critical values. The analysis of mixing under subcritical conditions is based on the assumption that there is a defined border between the liquid being injected and the surrounding gas. Hence, it is safe to assume that the liquid density is nearly constant and is limited by the boiling temperature. The supercritical mixing process exhibits many characteristics distinct from those in a subcritical environment, thereby rendering conventional approaches developed for low pressure applications invalid (Yang 2000). In the supercritical regime, most of the previous interests were applied to the domain of subcritical injection into a supercritical environment (see for example Mayer *et al.* 1998; Chehroudi, Talley & Coy 2002; Oschwald *et al.* 2006; Segal & Polikhov 2008) driven by practical interests in rocket and diesel engine environments.

The supercritical regime is characterized by drastic changes in some important equilibrium properties of a pure substance as it approaches the thermodynamic critical point. The sharp distinction between liquid and gas phases disappears at and above the critical point, and the substance is more properly considered to be a fluid whose density can vary widely but continuously as temperature is changed at fixed pressure. Density changes can become particularly large near the critical point. Other properties that vary widely near the critical point are thermal conductivity and mass diffusivity.

† Email address for correspondence: arnab1985@ufl.edu

In addition, the constant pressure specific heat becomes very large and surface tension vanishes. Under true supercritical conditions, there cannot be evaporation since the latent heat is null, and a surface cannot exist. Therefore, the term 'emission rate' and 'emission constant' which are of more general meaning have been used often (Bellan 2000). For mixtures, the determination of critical conditions, called the 'critical mixing temperature or pressure' (critical lines for two-component mixture as opposed to a critical point for a pure substance) has a complex definition (Bruno & Ely 1991; Chehroudi 2006). In the remainder of the text, the terms subcritical and supercritical will refer to the critical condition of the pure substance used in the jet and not that of the mixture.

Although the data may present more interpreting difficulties binary or multiple species combinations where fluids emerge from an orifice into a chamber containing another fluid or mixture are more accurately descriptive of the situation in any combustion chamber. In this configuration, the distinction between jets and sprays is within the intent of the experiment. Jets are discussed when the intent is to study the fluid column disintegration, whereas sprays are discussed in the context of droplets that have already separated from the incoming fluid jet (Lin 2003; Baumgarten 2006). Similar to this, a distinction is made between atomization and disintegration, the former being a purely subcritical process and relies upon the existence of a surface that must break up, and the latter being a process that may occur whenever there is a boundary which may not be a tangible surface (Chehroudi *et al.* 2003).

The objective of this work was to analyse the mixing and jet disintegration process when the injectant initially at supercritical pressures was preheated beyond critical temperatures and injected into subcritical or supercritical chamber conditions. Here, the possibility exists, and indeed it was observed experimentally, that moving from supercritical-into-supercritical to a supercritical-into-subcritical combination, heat transfer leads to the re-establishment of injectant surface tension and drop formation was observed at a certain distance downstream of the injector. This thermodynamic system exists in practice for hypersonic applications hence it is of significant interest (Wu *et al.* 1999; Lin, Cox-Stouffer & Jackson 2006). Although the focus here was on supercritical-into-subcritical injection it was considered important to show also cases of supercritical-into-supercritical using the same experimental method and analysis to identify the transition from one regime to another. Extensive experiments were conducted to determine the influence of different parameters on the average droplet size for some given test conditions. Droplet size and formation locations were quantified. Planar laser-induced fluorescence (PLIF) was used through the jet centre plane with non-resonant excitation to visualize the gas-jet interface, the jet core and droplet formation up to 20 jet diameters downstream of the injector.

2. Experimental setup

The details of the setup were given previously (Segal & Polikhov 2008; Roy & Segal 2010), hence only a brief description is included here. The high-pressure chamber shown in figure 1 is constructed to withstand pressures up to 70 atm and temperatures up to 600 K. The thermocouples and pressure transducers used had an accuracy of ± 1 K and ± 10 kPa, respectively. For optical access there are three windows in the chamber which provide a field of view that is 22 mm wide and 86 mm long. All experiments were done using a round liquid injector with a diameter D of 2.0 mm and a length-to-diameter ratio of 10. FK-5-1-12 [$CF_3CF_2C(O)CF(CF_3)_2$] or 'fluoroketone' has been chosen as the injected fluid for its spectroscopic properties

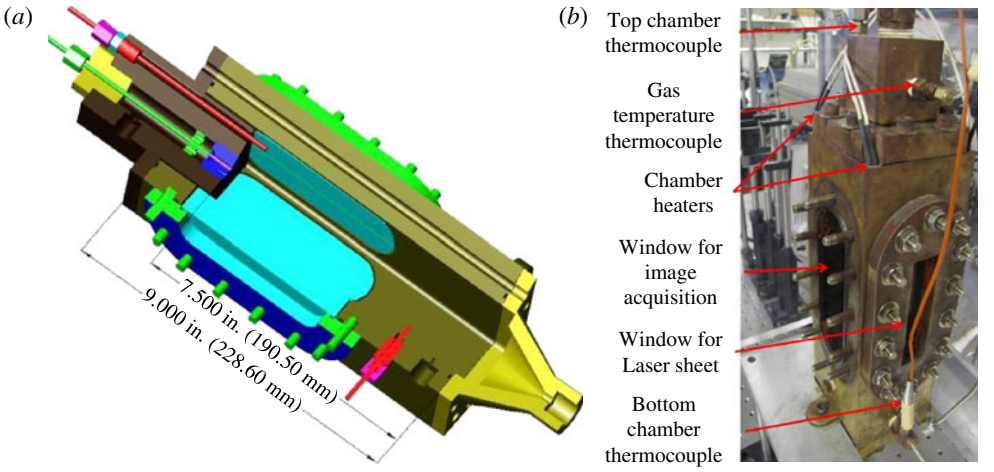

FIGURE 1. (Colour online) Test chamber schematic (*a*) and its overall view (*b*). The liquid and gas injection ports are at the top of the chamber. The chamber can be heated and pressurized to 600 K and 70 atm, respectively. Two of the four chamber heaters are shown. The injector diameter is 2 mm.

and low critical point ($P_{cr} = 18.4$ atm, $T_{cr} = 441$ K). Nitrogen has been chosen as the medium into which fluoroketone is injected. The third harmonic of Nd:YAG laser was used to excite the fluorescence. Earlier tests have shown that emission spectrum of fluoroketone within 400–500 nm does not reveal significant dependence on pressure and temperature within a range of interest (Gustavsson & Segal 2003). Based on emission spectra an optical filter with 420 nm centreline and 10 nm full width at half maximum (FWHM) is placed before the Princeton Instruments Intensified CCD camera lens to eliminate any elastic scattering. The ICCD Camera has a resolution of 1024 × 1024 pixels, but was cropped to 381 × 1024 pixels to increase the acquisition rate to 10 Hz and to synchronize it with the laser. The region of interest captured was 14 mm wide and 40 mm long, which corresponds to an axial length-to-jet diameter ratio (x/D) of 20 and a minimum detectable drop diameter of 40 μm. The gate width was fixed at 150 ns in order to capture the entire duration of fluorescence while reducing the background light significantly. A laser sheet of 0.1 mm thickness and 40 mm length was focused on the jet centreline to ensure that two-dimensional images were captured accurately. A detailed laser correction method was undertaken to account for the laser intensity loss through the different phases of fluoroketone. This complex calibration has been discussed in detail in an earlier work (Roy, Gustavsson & Segal 2011) and has been used in all of the current experiments for absorption of the laser sheet through the jet.

3. Experimental conditions

The experimental conditions are shown in figure 2 on a reduced pressure ($P_r = P/P_{cr}$) and reduced temperature ($T_r = T/T_{cr}$) diagram. The goal was to span a range of pressures and temperatures with particular focus around the critical point. Chamber and injectant conditions have been marked separately. Previous studies (Mayer *et al.* 2001; Chehroudi *et al.* 2003) have shown that supercritical behaviour may be encountered even when only one of the parameters, P_r or T_r, is critical. It was

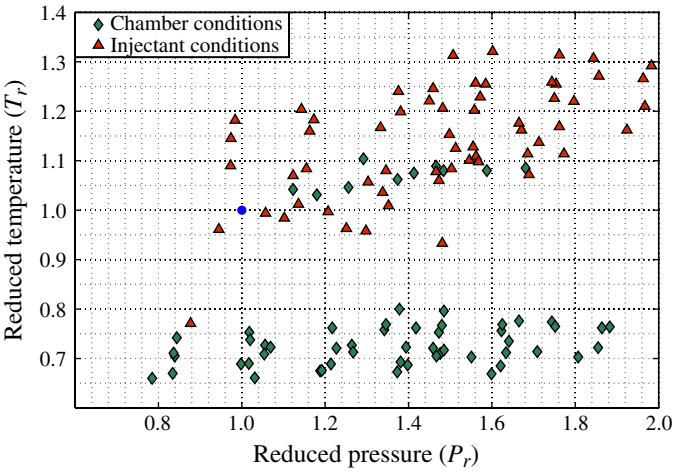

FIGURE 2. (Colour online) Selection of the experimental conditions. Reduced temperatures and pressures have been selected to cover the subcritical to supercritical regime. The plot indicates both the chamber and the injectant conditions independently.

Case	$T_{r,ch}$	$T_{r,inj}$	$P_{r,ch}$	$P_{r,inj}$	$\dot{m}$ (g s^{-1})	U_{inj} (m s^{-1})
1	0.69	1.13	1.38	1.51	19.31	20.98
2	0.72	1.21	1.86	1.97	18.33	17.95
3	0.76	1.29	1.88	1.98	17.24	20.31
4	0.80	1.31	1.38	1.51	16.99	30.00
5	1.04	1.00	1.26	1.34	17.82	7.07
6	1.06	1.08	1.37	1.47	16.78	14.56
7	1.08	1.08	1.41	1.50	17.35	14.47
8	1.09	1.18	1.47	1.67	18.64	20.57

TABLE 1. Selected test cases.

observed in this study that both parameters need to exceed the critical values for complete supercritical behaviour to exist. Hence, the term 'supercritical' here shall be referred to cases where both temperature and pressure are supercritical, while 'subcritical' shall be referred to cases where only the temperature is subcritical. The highest pressures tested were nearly $2P_r$, i.e. 37 atm, while the highest temperatures tested were $1.35T_r$, i.e. 583 K. This was done to ensure that supercritical conditions were achieved even if the mixture effects shifted the critical point.

4. Results and discussion

Supercritical injection into subcritical and supercritical environments show clear differences in jet disintegration and gas-jet interface appearance. A few selected test conditions have been listed in table 1 where the subscripts '*ch*' and '*inj*' designate the chamber and the injectant, respectively, while $\dot{m}$ is the injection mass flow rate. The first four cases represent supercritical-into-subcritical injections, while the last four represent supercritical-into-supercritical injections. For all of the tests, the mass flow rate was kept relatively constant. Differences in injection velocity U_{inj} existed

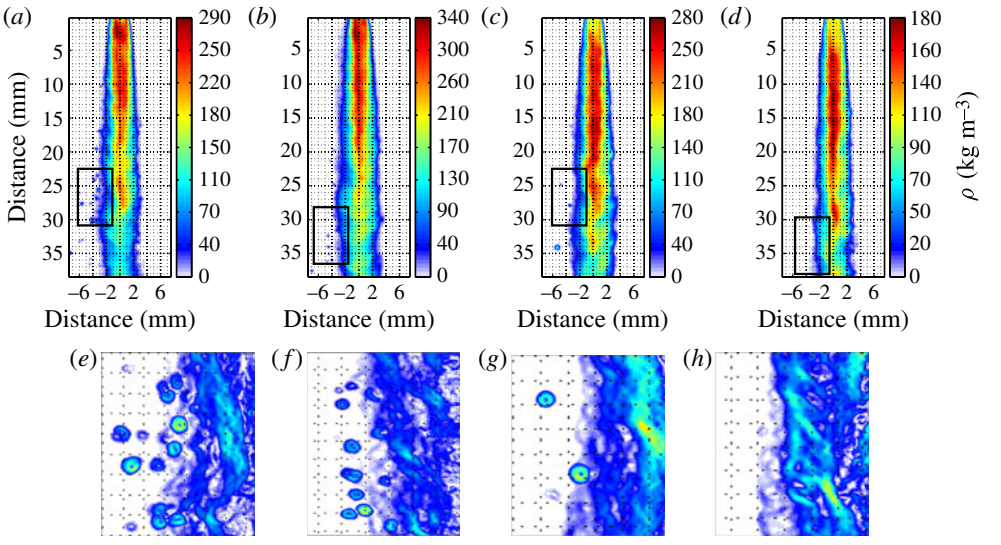

FIGURE 3. (Colour online) Scaled images of a supercritical jet injected into subcritical chamber conditions. Test conditions correspond to cases 1–4 in table 1: (*a–d*) density images; (*e–h*) zoomed-in density gradient images.

due to large changes in density near the critical point, and it ranged between 3 and 30 m s^{-1}. Pressures were maintained supercritical for all test conditions to isolate the effects of temperature in the disintegration and mixing processes. Buoyancy effects are negligible compared with the inertial forces for all of the test cases mentioned. This was verified by a length scale x_b based on Froude number Fr defined as $x_b = Fr^{-1/2}\,(\rho_{inj}/\rho_{ch})^{-1/4}(x/D)$ where $Fr = \rho_{inj}U_{inj}^2/gD(\rho_{inj} - \rho_{ch})$. Earlier works (Chen & Rodi 1980; Papanicolaou & List 1988) have shown that the flow is momentum dominated if $x_b < 0.53$. This criterion was found to be true for all of the current experiments where the average value of $x_b = 0.20$.

4.1. *Supercritical injection into a subcritical atmosphere*

In these test cases, the fluid was preheated to supercritical temperatures before injection into the chamber which was maintained at subcritical conditions. Both were at supercritical pressures. Representative test cases 1–4 have been listed in table 1. The cases have been chosen such that chamber and injectant temperatures are in increasing order of magnitude. Figure 3 shows the respective images of the listed test cases. Density images have been shown on the first row from figure 3(*a–d*), while zoomed-in density gradient images of the gas–jet interface are shown below the corresponding density images from figure 3(*e–h*).

Since the fluid is in a supercritical state when it is being injected, the surface tension effects are negligible in the initial mixing region, which is very close to the injector at around 5–10 injector diameters. Typical characteristics of supercritical injection are noted in this region, including a smooth jet–gas interface and occasional formation of 'ligaments' and clusters. Further downstream of the injector, the jet interface changes. In case 1 or figure 3(*a*) it can be seen that several droplets form beyond 10 injector diameters from the injector and detach from the main body of the jet. This is due to the heat transferred from the jet as it is injected into a significantly cooler medium,

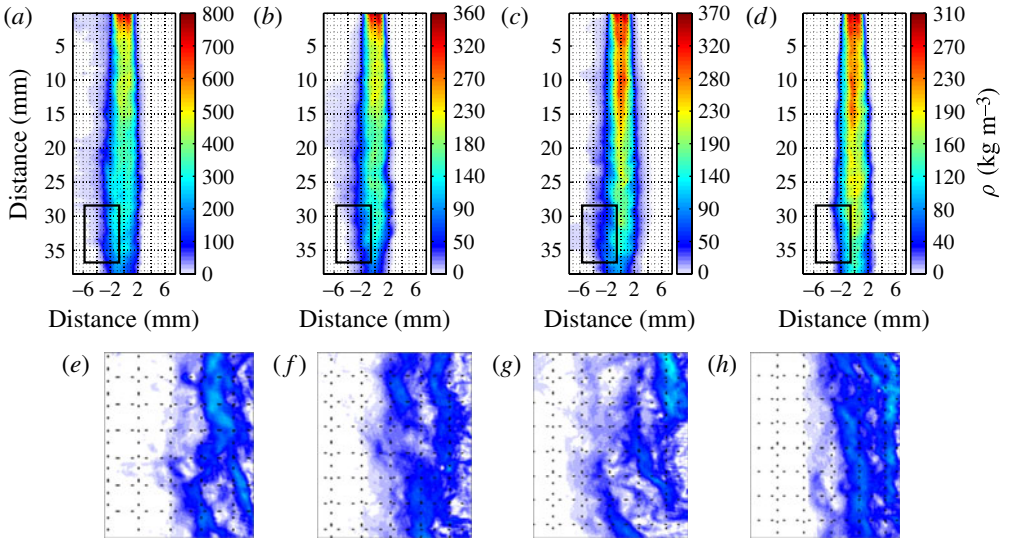

FIGURE 4. (Colour online) Scaled images of a supercritical jet injected into supercritical chamber conditions. Test conditions correspond to cases 5–8 in table 1: (*a–d*) density images; (*e–h*) zoomed-in density gradient images.

and hence the conditions become locally subcritical. Any portion of the jet that breaks off will cool below the critical temperature and form spherical droplets due to surface tension forces gaining importance. This effect is most prominent in the first two cases, where the temperature of the chamber is the lowest, causing the greatest heat transfer. The temperature of the surrounding environment gradually increases from figure 3(*a*) through to figure 3(*d*) and droplets gradually disappear since local conditions are not cool enough to cause subcritical phenomena to exist. Density gradient values also gradually decrease due to the increase in temperature of both the surroundings and the injectant.

4.2. *Supercritical injection into a supercritical atmosphere*

To compare the differences in the gas–jet interface appearance and the breakup process with those of the previous section, supercritical fluid was injected into a supercritical environment. Representative test cases 5–8 have been listed in table 1 in increasing order of chamber and injectant temperatures and pressures. Figure 4 shows the respective images of the listed test cases as in the earlier case. Density images have been shown on the first row from figure 4(*a–d*), while the respective zoomed-in density gradient images of the gas–jet interface are shown from figure 4(*e–h*).

The fluid in these injection conditions exhibit complete supercritical behaviour. Figure 4(*a–d*) show no effects of surface tension or droplet formation as far as 20 jet diameters from the injector even at lower chamber temperatures. There are some finger-like entities that emerge from the jet but do not break up into droplets as the previous case. The images progressively resemble the injection of a gaseous turbulent jet into a gaseous environment with increasing temperatures and pressures as observed by other researchers (Mayer *et al.* 1998; Chehroudi *et al.* 2002; Oschwald *et al.* 2006). This is clearly demonstrated in figure 4(*e–h*) where the gas–jet interface has been zoomed in. The density-gradient magnitudes also continue to decrease.

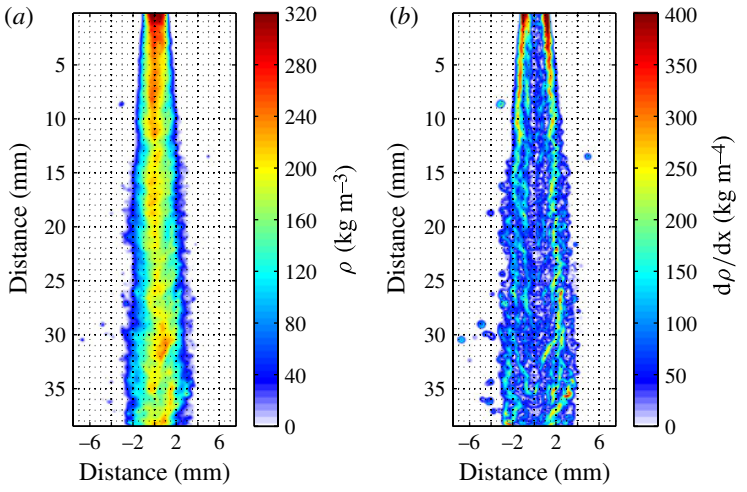

FIGURE 5. (Colour online) Drop formation increases with distance from injector plane. Experimental conditions are: $T_{ch} = 19\,^{\circ}\mathrm{C}$, $T_{inj} = 192\,^{\circ}\mathrm{C}$, $P_{ch} = 21.9$ atm, $P_{inj} = 32.9$ atm and $U_{inj} = 19.2$ m s^{-1}. Density and density gradient images are shown in (*a*,*b*), respectively.

The last two sets of images in figure 3, i.e. figure 3(*c*,*d*), show resemblance to the second wind-induced breakup regime according the classical breakup theory (Reitz & Bracco 1982; Lin & Reitz 1998). When the conditions approach supercritical values for the chamber, the jet gradually begins to take the appearance of a gas jet without entering the atomization regime as seen in figure 4. This departure from the classical jet breakup behaviour occurs due to the reduction of surface tension and the heat of vapourization to a near-zero value at and above the critical point. The mixing process is enhanced drastically in this regime since the behaviour is more like gas–gas mixing. In the supercritical-into-subcritical cases, the formation of droplets indicates the need for vapourization of the same in order to efficiently mix with the surroundings, and hence directly affecting the combustion efficiency.

4.3. *Analysis of drop formation and size*

The concept of jet disintegration was first suggested by Rayleigh (1879) based on the energetic instabilities of a cylindrical jet which analytically lead to a characteristic drop diameter $d_d = 1.89d_l$ during the breakup process. This value was close to the experimental results of Taylor & Hoyt (1983) who found $d_d = 1.92d_l$. Additional theoretical and experimental works including the effects of jet viscosity and the influence of the surrounding gas resulted in semi-empirical expressions to predict the droplet size distribution as well as the jet breakup length, for example, see Sterling & Sleicher (1975).

Owing to the disappearance of the surface tension, droplet formation is no longer possible under supercritical conditions which is evident from the images shown in figure 4 for the supercritical injection into a supercritical environment cases. However, for the supercritical injection into a subcritical environment, the reassertion of surface tension occurs as the fluoroketone cools. An example is shown in figure 5 where it can be seen that the drop population increases with the distance from the injection.

The formation of drops was quantified using a 'no drop parameter' or *NDP* that indicated whether or not any drop would be produced. This was defined as the product

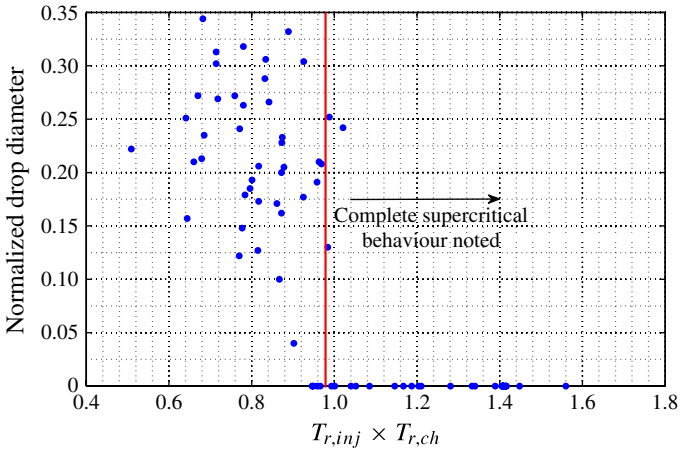

FIGURE 6. (Colour online) Plot of the *NDP*. No supercritical-to-subcritical transition was found for $NDP > 0.975$ and therefore no droplet is formed.

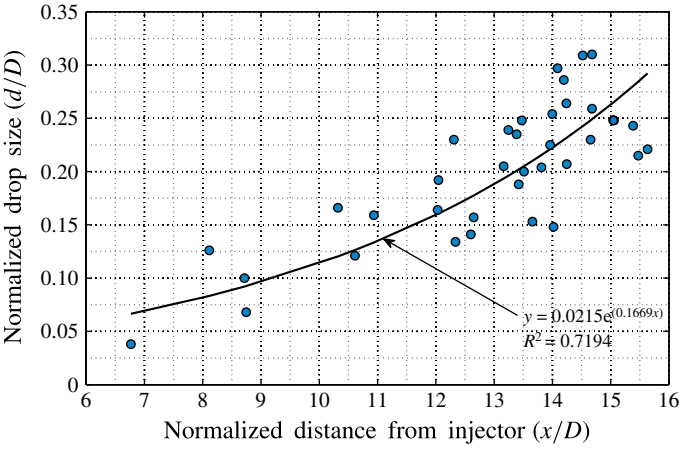

FIGURE 7. (Colour online) Plot of the average drop size against the average distance from the injection. An exponential curve is fitted to the data points with a RMSE of 0.04.

of the jet and environment reduced temperatures:

$$NDP = T_{r,ch} \times T_{r,inj} = \frac{T_{ch} \times T_{inj}}{T_{cr}^2}. \tag{4.1}$$

It was found that when $NDP > 0.975$ and pressures are always supercritical, no droplet formation is observed. This can be seen in figure 6 where the average drop diameter normalized by the injector diameter is plotted against *NDP*.

The drop sizes were quantified as a function of temperature combination, a measure of the amount of heat transferred, and also as a function of the distance from the injector location, a measure of temporal effects. These results are shown in figure 7, where both quantities plotted have been normalized using the injector diameter. Each test case consists of around 15 images that are used for drop size calculation, while

each image usually consists of about 5–10 drops. The total number of drops in each test case thus varies from 50 to 100, and the drop sizes are averaged accordingly. The plot indicates that the average droplet size increases exponentially with the distance from the injector with a mean exponential coefficient of 0.1669. The root mean square error (RMSE) of the data points about the fitted curve is 0.04. These results reinstate the fact that as the supercritical jet penetrates into the cooler, subcritical gaseous environment, the surface tension forces increase drastically and the mixing transitions from a gas–gas regime as seen in supercritical-to-supercritical injections to a second wind-induced liquid breakup-type regime.

With the slowest injection velocities and the highest camera frequency used for the current experiments, the jet travels 0.3 m from the injector, which is an order of magnitude larger than the axial distance captured in each frame. Hence, averaging of images is implemented here. Additional effects that increase the uncertainty of the droplet size determination is the nature of the two-dimensional analysis which neglects the drops formed out of the laser sheet plane.

5. Conclusions

A study of a jet at supercritical conditions injected into subcritical and supercritical chamber conditions was undertaken. The images were obtained using PLIF through the jet centre plane. The images indicate the characteristics of subcritical and supercritical mixing as mentioned in the theories. Since pressures were always kept supercritical, temperatures of both the injectant and chamber were used in determining the state of the injected fluid.

In the case of a supercritical jet injected into a subcritical environment, droplets were observed to form at beyond 10 jet diameters downstream of the injector at lower chamber temperatures. This was due to the heat transferred from the jet to the surroundings and, hence, the existence of local subcritical conditions where surface tension gained importance. A gradual increase of chamber temperature inhibited the formation of drops and the jet–gas interface became smoother. In the case of a supercritical jet injected into a supercritical environment, the jet surface exhibited complete supercritical behaviour with no formation of droplets noted. Surface tension disappeared completely, and the surface became smooth with minimal irregularities. With increased temperature and pressure, the density gradient values decrease and the jet resembled that of a turbulent gas jet injected into a gaseous atmosphere.

To predict the formation of droplets a ‘no drop parameter’ or *NDP* was used. It was observed that if the *NDP* was greater than 0.975, no drops were seen for up to 20 jet diameters in the axial direction. The average drop size was found to increase exponentially with the distance from the injector, indicating that the surface tension forces gradually become stronger as the supercritical jet penetrates into the cooler, subcritical atmosphere. It can thus be concluded that the mixing process is enhanced drastically in the supercritical-into-supercritical injection cases than the supercritical-into-subcritical cases since the formation of droplets in the latter indicates the need for vapourization of the same for efficient mixing, and hence directly affecting combustion efficiency.

REFERENCES

BAUMGARTEN, C. 2006 *Mixture Formation in Internal Combustion Engines*. Springer.

BELLAN, J. 2000 Supercritical (and subcritical) fluid behaviour and modeling: drops, streams, shear and mixing layers and sprays. *Prog. Energy Combust. Sci.* **26**, 329.

BRUNO, T. J. & ELY, J. F. 1991 *Supercritical Fluids: A Review in Modern Technology and Applications*. CRC.

CHEHROUDI, B. 2006 Supercritical fluids: nanotechnology and select emerging applications. *Combust. Sci. Technol.* **178**, 555–621.

CHEHROUDI, B., TALLEY, D. G. & COY, E. 2002 Visual characteristics and initial growth rates of round cryogenic jets at subcritical and supercritical pressures. *Phys. Fluids* **14**, 850–860.

CHEHROUDI, B., TALLEY, D., MAYER, W., BRANAM, R., SMITH, J. J., SCHIK, A. & OSCHWALD, M. 2003 Understanding injection into high pressure supercritical environments. In *Fifth International Symposium on Liquid Space Propulsion*. Huntsville, AL, NASA.

CHEN, C. J. & RODI, W. 1980 *Vertical Turbulent Buoyant Jets – A Review of Experimental Data*. Pergamon.

GUSTAVSSON, J. P. R. & SEGAL, C. 2003 Fluorescence spectrum of 2-trifluoromethyl-1,1,1,2,4,4,5,5,5,-nonafluoro-3-pentanone. *Appl. Spectrosc.* **61** (8), 984.

LIN, S. P. 2003 *Breakup of Liquid Sheets and Jets*. Cambridge University Press.

LIN, K. C., COX-STOUFFER, S. K. & JACKSON, T. A. 2006 Structure and phase transition processes of supercritical methane/ethylene mixtures injected into a subcritical environment. *Combust. Sci. Technol.* **178** (1).

LIN, S. P. & REITZ, R. D. 1998 Drop and spray formation from a liquid jet. *Annu. Rev. Fluid Mech.* **30**, 85–105.

MAYER, W., IVANCIC, B., SCHIK, A. & HORNUNG, U. 1998 Propellant atomization in LOX/GH2 rocket engines. In *34th Joint Propulsion Conference and Exhibit*. AIAA.

MAYER, W., TELAAR, J., BRANAM, R. & SCHNEIDER, G. 2001 Characterization of cryogenic injection at supercritical pressures. In *37th Joint Propulsion Conference and Exhibit*. AIAA.

OSCHWALD, M., BRANAM, R., HUSSONG, J., SCHIK, A., CHEHROUDI, B. & TALLEY, D. G. 2006 Injection of fluids into supercritical environments. *Combust. Sci. Technol.* **178**, 49–100.

PAPANICOLAOU, P. N. & LIST, E. J. 1988 Investigations of round vertical turbulent buoyant jets. *J. Fluid Mech.* **195**, 341–391.

RAYLEIGH, LORD 1879 On the instability of jets. *Proc. Lond. Math. Soc.* **10**, 4–13.

REITZ, R. D. & BRACCO, F. V. 1982 Mechanism of atomization of a liquid jet. *Phys. Fluids* **25**, 1730–1742.

ROY, A., GUSTAVSSON, J. P. R. & SEGAL, C. 2011 Spectroscopic properties of a perfluorinated ketone for PLIF applications. *Exp. Fluids* **51** (6), 1451–1463.

ROY, A. & SEGAL, C. 2010 Experimental study of fluid jet mixing at supercritical conditions. *J. Propul. Power* **26** (6), 1205–1211.

SEGAL, C. & POLIKHOV, S. A. 2008 Subcritical to supercritical mixing. *Phys. Fluids* **20** (5), 052101–052107.

STERLING, A. M. & SLEICHER, C. A. 1975 The instability of capillary jets. *J. Fluid Mech.* **68**, 477–495.

TAYLOR, J. J. & HOYT, J. W. 1983 Water jet photography - techniques and methods. *Exp. Fluids* **1**, 113.

WU, P., SHAHNAM, M., KIRKENDALL, K. A., CARTER, C. & NEJAD, A. 1999 Expansion and mixing processes of underexpanded supercritical fuel jets injected into superheated conditions. *J. Propul. Power* **15** (5), 642–649.

YANG, V. 2000 Modeling of supercritical vaporization, mixing and combustion processes in liquid-fueled propulsion systems. *Proc. Combust. Inst.* **28**, 925.